LASER ASSISTED GROWTH OF SILICON NANO-STRUCTURES

by

Elif Demirbaş

Bachelor of Science, Physics, Boğaziçi University, 2008

Submitted to the Institute for Graduate Studies in
Science and Engineering in partial fulfillment of
the requirements for the degree of
Master of Science

Graduate Program in Physics
Boğaziçi University

2010

ACKNOWLEDGEMENTS

I would like to express my appreciation to Professor Naci İnci for submission of the subject, for his suggestions in the development of this study, for his invaluable guidance and help in an empathic manner and for his motivation during the preperation of this dissertation.

I would like to thank Dr.Bükem Bilen and Mrs.Aslı Çakır Saygılı for their guidance at the beginning of the experimantal study.

I would like to express my sincere gratitude to Mrs.Sabriye Açıkgöz for her kind and precious guidance and her talented support during all steps of this study.

I would like to thank Mr.İbrahim Sarpkaya for his worthy opinions, suggestions and support for the final editions of this thesis.

Thank Mr.Veli Uğur Güney for his assist of preparing this thesis and my defence presentation.

I would like to appreciate to Miss.Emine Ertuğrul for her kind and invaluable support and motivation.

I would like to state my special thanks to my whole family for their appreciable support and endeavours.

ABSTRACT

LASER ASSISTED GROWTH OF SILICON NANO-STRUCTURES

In this study, the aim is to produce homogeneous porous silicon(PS) nano-structures and then to observe the effect of resistivity of starting silicon samples. P-type silicon wafers with different resistivity are prepared by different anodization methods. Silicon samples fabricated by the electrochemical dissolution are characterized both optically and structurally. By the highlight of quantum confinement effect, optical characterization method is used to determine whether porous silicon nano-structures occur or not. Porous silicon samples are analysed by the Environmental Scanning Electron Microscopy(ESEM).

ÖZET

SİLİKON NANO-YAPILARIN LAZER YARDIMIYLA BÜYÜTÜLMESİ

Bu çalışmadaki amaç, öncelikle homojen gözenekli silikon nano-yapılar oluşturmak, daha sonra silikon örneğinin direncinin etkisini gözlemlemektir. Farklı dirençlerdeki p tipindeki silikon tabakalar, farklı anotlama yöntemleri ile hazırlanmıştır. Elektrokimyasal çözünme ile üretilen silikon örnekleri optik ve yapısal olarak analiz edilmiştir. Kuantum kısıtlama etkisinin ışığında, gözenekli silikon nano-yapıların oluşup oluşmadığnı belirlemek için optik tanımlama yöntemi kullanılmıştır. Gözenekli silikon örnekleri ESEM(Çevresel Taramalı Elektron Mkroskobu) tarafndan incelenmiştir.

TABLE OF CONTENTS

LIST OF FIGURES

LIST OF SYMBOLS/ABBREVIATIONS

AFM	Atomic Force Microscope
BDF	Band Pass Filter
EHP	Electron Hole Pair
ESEM	Environmental Scanning Electron Microscope
HF	Hydrofluoric Acid
HPF	High Pass Filter
PL	Photoluminescence
PS	Porous Silicon
SEM	Scanning Electron Microscope

1. INTRODUCTION

The discovery of room-temperature photoluminescence(PL) of porous silicon(PS) has initiated an extensive research on both theoretical and experimental aspects, especially because of its strong potential in its use in optoelectronic and photonic applications. Porous silicon has a very wide, practical applications. Porous silicon can be the basis of medical, optoelectronic and photonic devices. Porous silicon microneedle array is used to deliver drug into the human body. This is used to the people especially with cancer in order not to be pained [1]. As an photonic device, in the solar cells, porous silicon is used due to its efficient luminescence [2]. Ligth emitting diodes also can be prepared by the help of the luminescence of porous silicon [3]. In addition, porous silicon is used for the lifetime inhibitions.

Fabrication of PS samples can be performed by electrochemical anodization, stain etching and chemical vapor decomposition. There are many parameters affect the formation of porous silicon structure such as resistivity, current density, anodization time and drying conditions.

From the discovery of the photoluminescence property of porous silicon to today, there have been many studies to form regular, homogeneous nano-pores and pillars [4].

The purpose of this study is to examine the optical and structural properties of porous silicon nano-structures which have been achieved by electrochemical anodization of p-type silicon wafers having different resistivities. As a consequence, to achieve homogeneous nano-pillars on the silicon surface and to see the effects of the resistivity on PS nano-structure formation is intended.

The layout of the thesis is given in the the following sequence; information about the techniques which are used to produce porous silicon, effecting parameters, pore initiation, quantum confinement effect, luminescence and single-mode and multi-mode laser is given in chapter 2. In chapter 3, experimental procedure of PS sample, optical

and structural characterization methods are intrduced. Furthermore, results which are obtained from photoluminescence(PL) spectroscopy, environmental scanning electron microscopy(ESEM) are analysed. Finally, in chapter 4, conclusion is given.

2. REVIEW

2.1. Techniques on Growth Mechanism of Porous Silicon

The formation of porous silicon(PS) is attained by two different ways. One of these ways is anodization method, the other one is stain etching. In the anodization method, pores can be formed by the use of anodization cell. In the anodization cell, there is an hidrofluoric(HF) acid and ethanol solution that dissolves silicon wafers electrochemically [5]. Ethanol is used, because ethanol prevents porous silicon from the stick of Hydrogen bubbles which is generated during the anodization. The basic anodization cell is shown in the Figure 2.1. In the basic anodization cell, silicon wafer and a HF-resistant are used as anode and cathode, respectively. Platinum or stainless steel can be used as the HF-resistant. Although this basic anodization cell has the advantages of simplicity, it has some inconsistencies. The decreasing current density across the silicon wafer across the silicon wafer can be count as one of these inconsistencies. Therefore, non-uniform current density results in the inhomogeneity of formed pores and the different surface thickness of porous silicon [4].

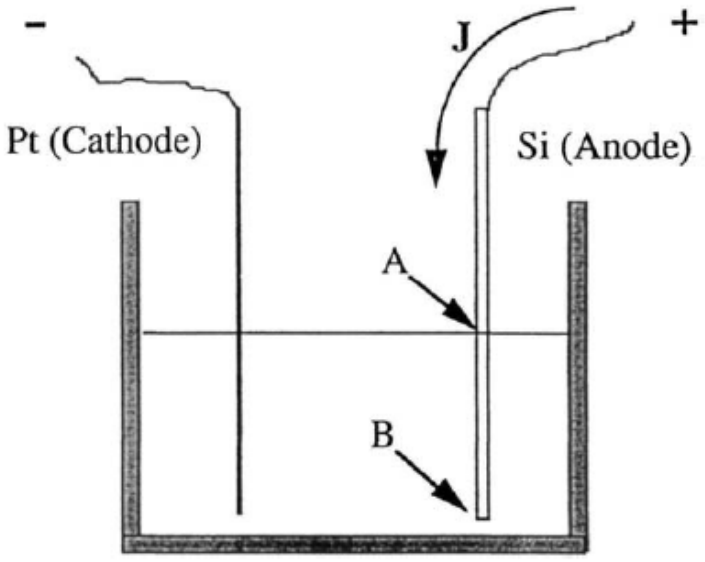

Figure 2.1. Cross-sectional view of the basic anodization cell

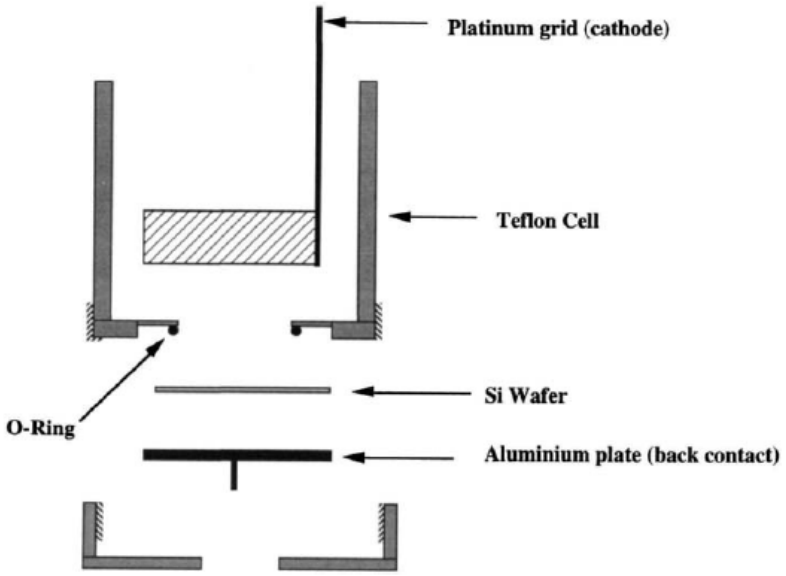

Figure 2.2. Single tank cell

A single tank cell which is shown in Figure 2.2 is the second type of the anodization cell. The elements of the single tank cell are the teflon cell, the O-ring, platinum grid and aluminum plate. The silicon wafer is positioned over the O-ring which is placed over the bottom hole of the inverted teflon cell. The platinum grid and copper plate is connected to the negative and positive terminals of the power supply, respectively. After converting the teflon cell upright, HF ethanol solution is poured into the cell [6]. In this type anodization, whole surface of the silicon wafer is exposed to HF. This leads to the uniform pore formation. Also, resistivity of silicon play a great role on the back-side contact. For highly resistive silicon wafer, high dose back contact is needed for homogeneous pore formation. However, for the silicon wafers which has low resistivity, uniform pores is attained without metallic contact. The single tank cell is commonly prefered because of its advantages [4].

The double tank cell is the other type of anodization. As shown in the Figure 2.3, it consists of two half-cells in which platinum electrodes are put into the HF solution and the silicon wafer seperates and isolates the two half-cells [7]. In this case, both side of silicon is exposed to the HF solution. The two Pt electrodes are connected to a power supply. The current comes from the positively connected Pt electrodes to the

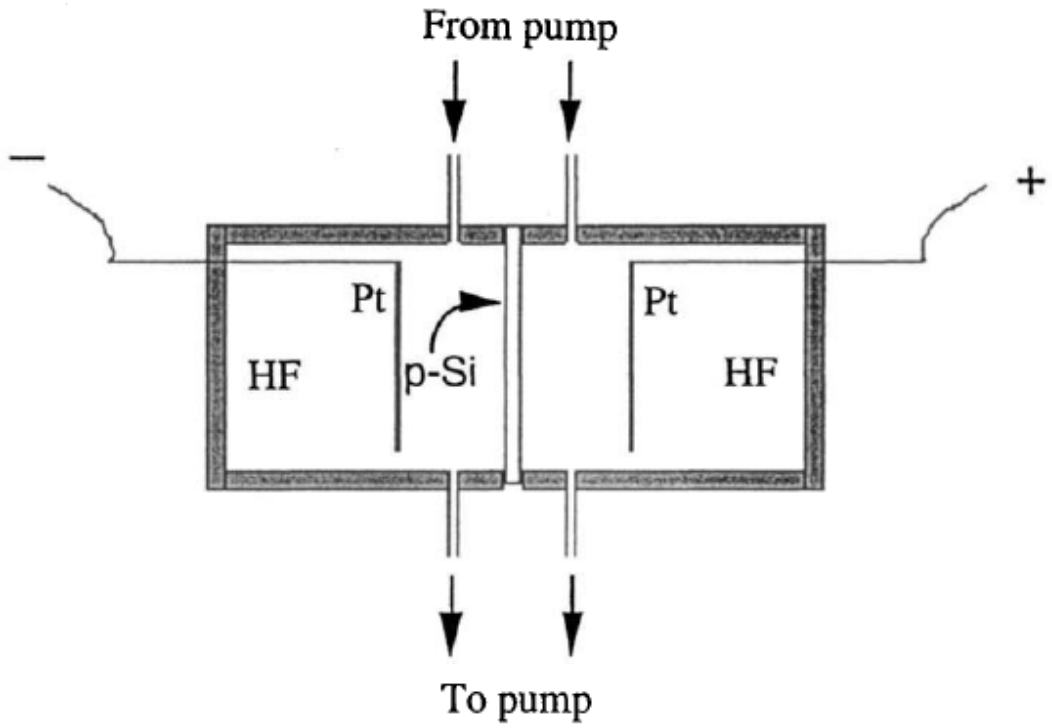

Figure 2.3. Double Tank Cell

back side of the silicon wafer which behaves like a cathode. Then the current flows through the other side of silicon and the negatively connected Pt electrodes. Porous silicon occurs at the front size of silicon wafer. Hydrogen bubbles generated during the anodization are removed from the cell by the help of chemical pumps [4].

Stain etching is the another technique used for porous silicon formation. Chemical stain-etch is consisted essentially of HF, nitric acid and water. Although the stain-etching process is easier method, it is performed less frequently. Because it has some disadvantages such as low photoluminosity and non-uniform pore structures [4].

2.2. Effecting Parameters

Porous silicon formation is not a simple process. It is initiated and continued by some parameters. Some of these significant parameters can be listed as resistivity, current density, anodization time and drying conditons.

2.2.1. Resistivity of Silicon Wafers and Operating Current Density(J)

Resistivity of the starting samples plays a key role in the formation of porous silicon. How much a material opposes the flow of electric current is the electrical resistivity(ρ) which is given by Equation 2.1,

$$\rho = \frac{E}{J} \tag{2.1}$$

where ρ is the electrical resistivity, E is the magnitude of the electric field, J is the magnitude of the current density.

The electrical resistivity ρ can also be given by

$$\rho = \frac{RA}{l} \tag{2.2}$$

where ρ is the electrical resistivity, R is the electrical resistance, l is the length of the material and A is the cross-sectional area of the material.

The electrical resistivity is also defined as the inverse of the conductivity of the material.

$$\rho = \frac{1}{\sigma} \tag{2.3}$$

Resistivity of the silicon samples and the operating current density(J) are related to each other. In the semiconductor materials, the current density(J) is written as

$$J = q(n\mu_n + p\mu_p)E \tag{2.4}$$

where q is the the charge of the electron, n and p are the electron and hole concentration, respectively. μ_n and μ_p are the electron and hole mobility, respectively [3].

2.2.2. Anodization Time and Drying Conditions

Porosity of the PS samples depends on anodization time and drying conditions. Anodization time affects both the thickness of the porous layer and porosity. Although there is a critical anodization time that gives the maximum porosity, porosity and anodization time are related to each other linearly up to critical anodization time. Above the critical anodization time, porosity decreases. As the time passed, the porosity shows an oscillatory behaviours [14].

Moreover, drying conditions is very significant for the pore formation. During the drying stage of the sample, evaporization of the HF solution from the pores causes a stress which result in cracks at the surface of the PS. The various drying conditions are the supercritical drying, freeze drying, pentane drying and slow evaporation. The most efficient drying technique is supercritical drying, but is expensive and difficult to perform. When the sample is frozen at a temperature around -500 F and the sublimation property of liquid drives the process, then this drying technique called as freeze drying. Pentane drying is the technique which uses the pentane as the drying liquid instead of water. In the slow evaporating technique, water or ethanol is used [4].

2.3. Pore Initiation

Porous layer formation initiaited by pit formation. Pits are formed by the breakdown of the deep-depletion layer. Initial pits develop at dislocations and radial pore growth occurs by the improvement of the electric field at the space-charge-layer boundary [8]. The electrochemical dissolution of silicon includes the transfer of several charges. The reaction rate is associated with the first hole supplied to the surface. Hole transfer to the interface depends on the band bending $e\phi$ and a characteristic diffusion velocity

$$V_D = \mu_p E_s \tag{2.5}$$

where μ_p is the hole mobility and E_s is the surface electric field [10]. In the equilibrium macropore formation, a steady-state condition is assumed at the pore tips. The charge transfer due to holes exactly balances the availability of ions in the electrolyte. In such a case, holes are consumed at the pore tips and the pores grow vertically downwards [11].

2.4. Quantum Confinement Effect

The quantum confinemet effect occurs when the diameter of the particle and the wavelength of the electron wave function are in the same magnitude [12].

When the confining dimension is large compared to the wavelength of the particle, this particle behaves like a free particle. During this state, the bandgap remains at its original energy due to a continuous energy state. However, as the confining dimension diminishes and reaches a certain limit, the energy spectrum becomes discrete and the bandgap energy E_g is increased as shown in the Figure 2.4. Thus, the bandgap depends on the size.

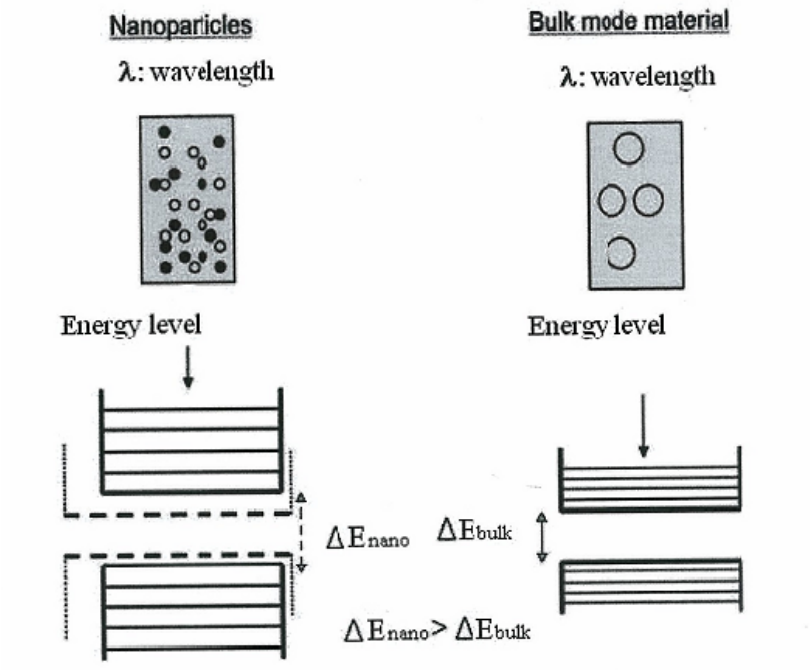

Figure 2.4. Quantum Confinement Effect

2.5. Luminescence

When an electron-hole pairs are generated in a semiconductor, or when carriers are excited into higher are generated in a semiconductor, or when carriers are excited into higher levels from which they fall to their equilibrium states, ligth can be given off the material. The general property of light emission is called luminescence. This overall category can be subdivided according to the excitation mechanism. If carriers are excited by photon absrption, the radiation resulting from the recombination of the excited carriers is called photoluminescence. If the excited carriers created by high-energy electron bombardment of the material, the mechanism is called cathodoluminescence. If the excitation occurs by the introduction of current into the sample, the resulting luminescence is electroluminescence [3]. The most important and lately invented one is the photoluminescence [4]. In the Figure 2.5, in the next page, shows the excitation and recombination mechanism in photoluminescence including a trapping level for electrons. When an incoming photon with energy larger than the band gap energy(E_g) is absorbed, it excites the electron in the valence band to the conduction band. By the excitation of the electron, a hole is created in the valence band. Therefore, the photon absorption yields an electron-hole pair(EHP)(a). The excited electron gives up energy to the lattice by scattering until it nears the bottom of the conduction band(b). The electron trapped by the impurity level E_t and remains trapped until it can be thermally reexcited to the conduction band(c, d). Direct recombination occurs as the electron falls to an empty state in the valence band, giving off a photon(e) [3].

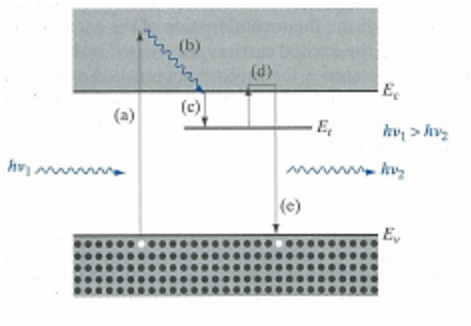

Figure 2.5. Excitation and recombination mechanisms in photoluminescence with a trapping level for electrons

2.6. Single-Mode and Multi-Mode Laser

Some important properties of laser diodes are determined by the geometry of the optical cavity. Generally, in the vertical direction, the light is contained in a very thin layer, and the structure supports only a single optical mode in the direction perpendicular to the layers and the laser known as single-mode laser. In the lateral direction, if the waveguide is wide compared to the wavelength of light, then the waveguide can support multiple lateral optical modes and the laser known as multi-mode laser [9].

3. EXPERIMENTAL STUDY AND RESULTS

3.1. Sample Growth

The starting samples are two kinds of p-type silicon, the first p-type silicon with 8-12 Ω.cm resistivity and the second one with 16-24 Ω.cm resistivity. Porous silicon samples are prepared by electrochemical anodization, both the basic anodization cell and the single tank cell. Silicon wafers are first cleaned using a methanol solution. Then, they are cut into pieces and back surface of the silicon pieces are coated with aluminum using PVD with Double Magnetron Sputtering System. Sputtering is a process which atoms are ejected from a solid target material because of the bombardment of the target by energetic particles as shown in Figure 3.1 [13].

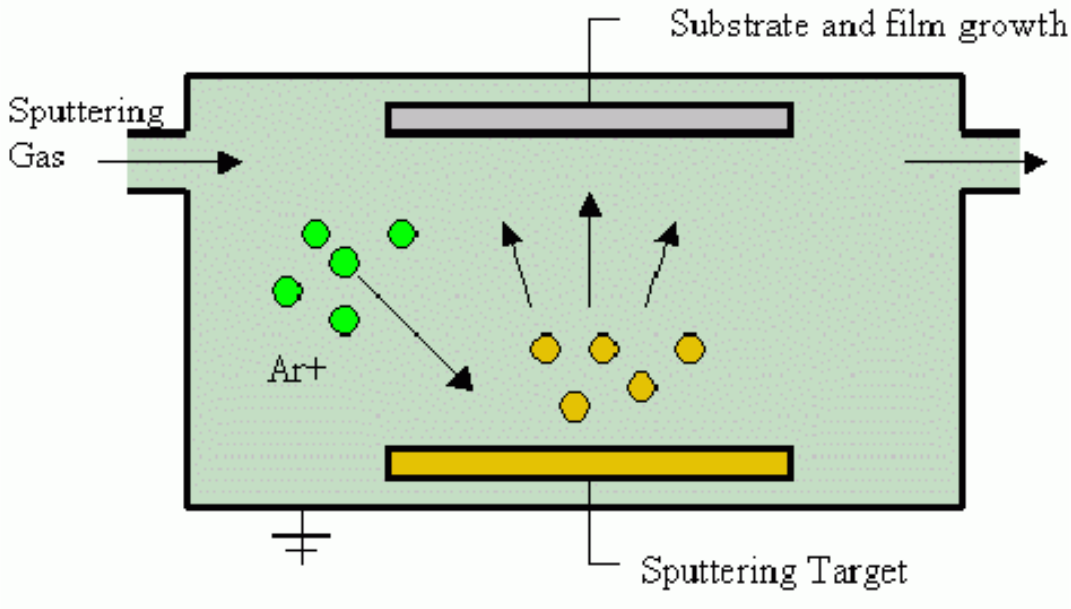

Figure 3.1. Magnetron Sputtering

The aluminum size will be coated can be adjusted by different masks while one mask has square holes with dimensions 1 cm by 1 cm, the other one has circular holes with 2,5 mm in diameter.

After aluminum coating, a copper wire is attached to aluminum part of the silicon samples by the help of silver paste. The back of the silicon samples are covered with wax

in order not to allow the copper wire to be exposed to HF. In the basic anodization cell, the silicon samples are dipped into HF ethanol(1:1) solution. The copper wire is connected to the positive terminal of the power supply and the stainless steel is connected to the negative terminal. In the second type of anodization, single tank cell, the copper wire of the silicon sample is extracted by the help of a hole at the bottom of the cell, the copper wire is connected to the positive terminal of the power supply. Then the ethanoic HF solution is poured into the cell. The stainless steel is again connected to the negative terminal of the power supply. The current density(J) is kept constant during both type of anodization. The operating current density, the resistivity of the silicon samples, the anodization time are very important parameters in producing regular pores and pillars and obtain well-packed photoluminescence spectra [14].

Samples are illuminted during anodization with Picoquant PDL 800-B Pulsed Diode Laser. While some of the silicon samples are illuminated by a multi-mode laser, some of them are illuminated by a single-mode laser. The aim of using multi-mode and single-mode laser is to observe the effect of different mode lasers on the formation of pillars and pores.

3.2. Optical Setup and Characterization

There are many type of optical characterization in order to analyse the samples. Some of optical characterization are listed as microscopy, ellipsometry, photoluminescence, cathodoluminescence and electroluminescence. In this work, porous silicon samples are analysed by the method of photoluminescence.

3.2.1. Photoluminescence Spectroscopy

A spectroscopy is an instrument used for measuring the intensity of light as a function of wavelength. Spectrometers usually contain a diffraction grating or prism to disperse the light, thereby spreading out the light of differing wavelengths into different positions.

The photoluminescence spectroscopy is shown in Figure 3.2. In this setup, an ultraviolet pulsed laser head with a wavelength of 405 nm is used in order to excite the electrons from porous silicon pillar tips. A picosecond diode laser(Picoquant PDL 800-B) drives this pulsed laser head. A dichroic mirror which is placed at 45^0 to the incident light reflects the excitation light towards a microscope objective(Nikon ELWD 50X). The excitation light is focused onto the sample. The excitation light is emitted from the sample and it goes through the dichroic mirror. Then, it is filtered out from two filters. Band-Pass Filter(BPF) and High-Pass Filter(HPF) are used to prevent any lost light from excitation beam. At the end, a fiber optic spectometer(USB4000-VIS-NIR Ocean Optics) is used to display the fluorescence emission.

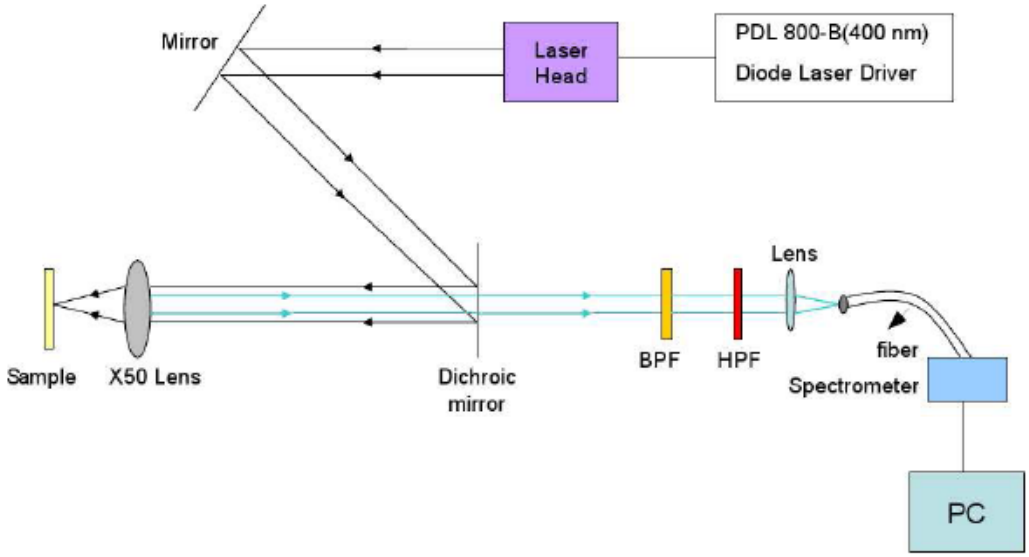

Figure 3.2. Optical setup of the photoluminescence spectroscopy

3.3. Structural Characterization

Structural characterization methods are Environmental Scanning Electron(ESEM) and Atomic Force Microscopy(AFM). AFM is generally used for measuring the thickness of very thin layer. In this work, ESEM is used for analyse the surface morphology of porous silicon samples.

3.3.1. Environmental Scanning Electron Microscopy

The scanning electron microscope(SEM) is a type of electron microscope that monitors the sample surface by scanning it with a high-energy beam of electrons. The electrons interact with the atoms that make up the sample producing signals that contain information about the sample's surface topography, composition and other properties such as electrical conductivity.

Figure 3.3. Picture of SEM chamber

Environmental Scanning Electron Microscopy accumulate the electric charge on the surfaces of non-metallic samples. In ESEM, the samples are placed in an internal chamber at higher pressure. The negative charge on the surface of sample is neutralized by the positively charged ions.

3.4. Results and Discussion

PS samples are characterized by the help of photoluminescence spectroscopy and environmental scanning electron microscopy. Photoluminescence experiment is performed for all PS samples in a dark room and at room temperature.

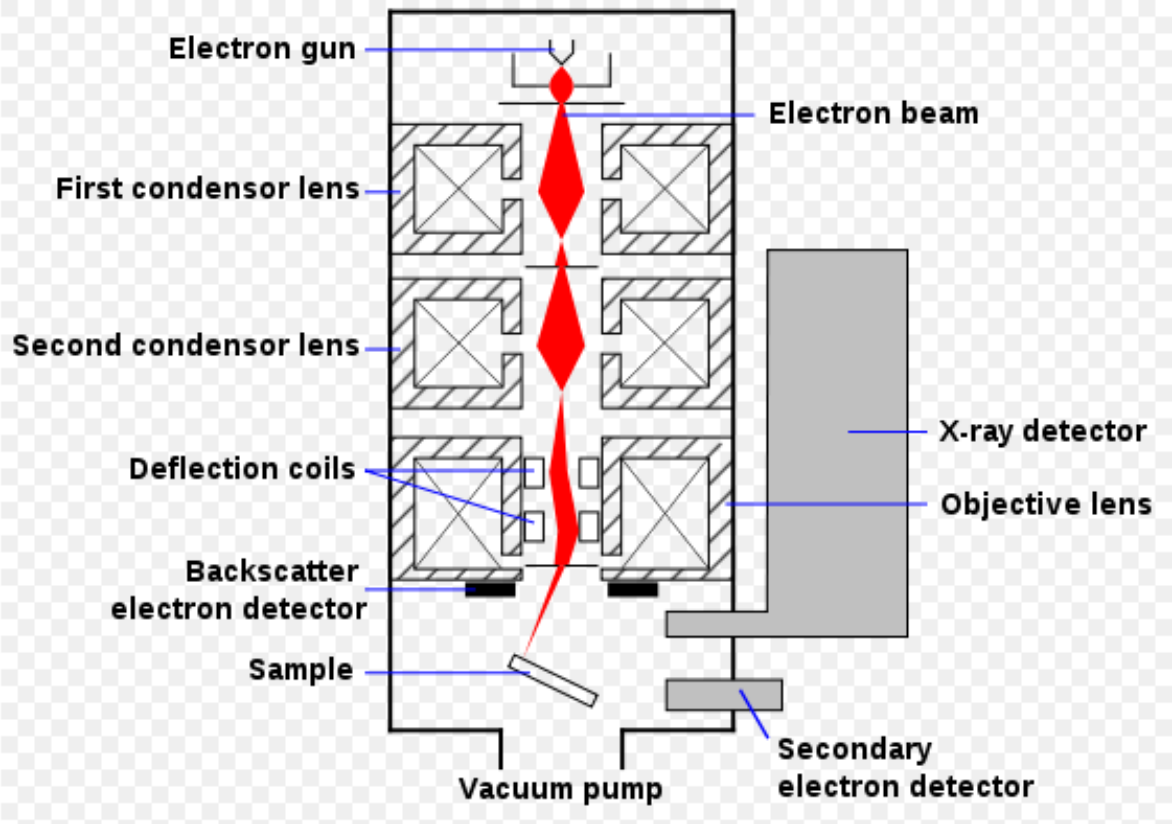

Figure 3.4. Schematic diagram of ESEM

Sample 10 shown in Figure 3.5 is prepared by the illumination of the multi-mode laser. Its structure determined by the ESEM shows that the pillars and pores are in the nanometer scale. Furthermore, according to its PL graph, intensity has a peak value at the wavelength of 675 nm(see Figure 3.9). However, sample H1 is prepared by the illumination of single-mode laser. Formed pillars are non-homogeneous and they do not have any tips. Also, we cannot get photoluminescence because of the quantum confinement effect.

In this thesis, especially, the aim is to show the effect of the resistivity on pores and pillar formation. The resistivity of starting sample are two kinds. PS sample fabricated from the silicon wafer with low resistivity has homogeneous pillar aray as seen in Figure 3.7. On the other hand, PS samples which are prepared by the high resistivity silicon wafer have not well-packed pillar aray and pores as shown in the Figure 3.8. Therefore, the resistivity of silicon has a great role on the formation of porous silicon. The growth of pillar is limited by the resistivity of silicon. This result

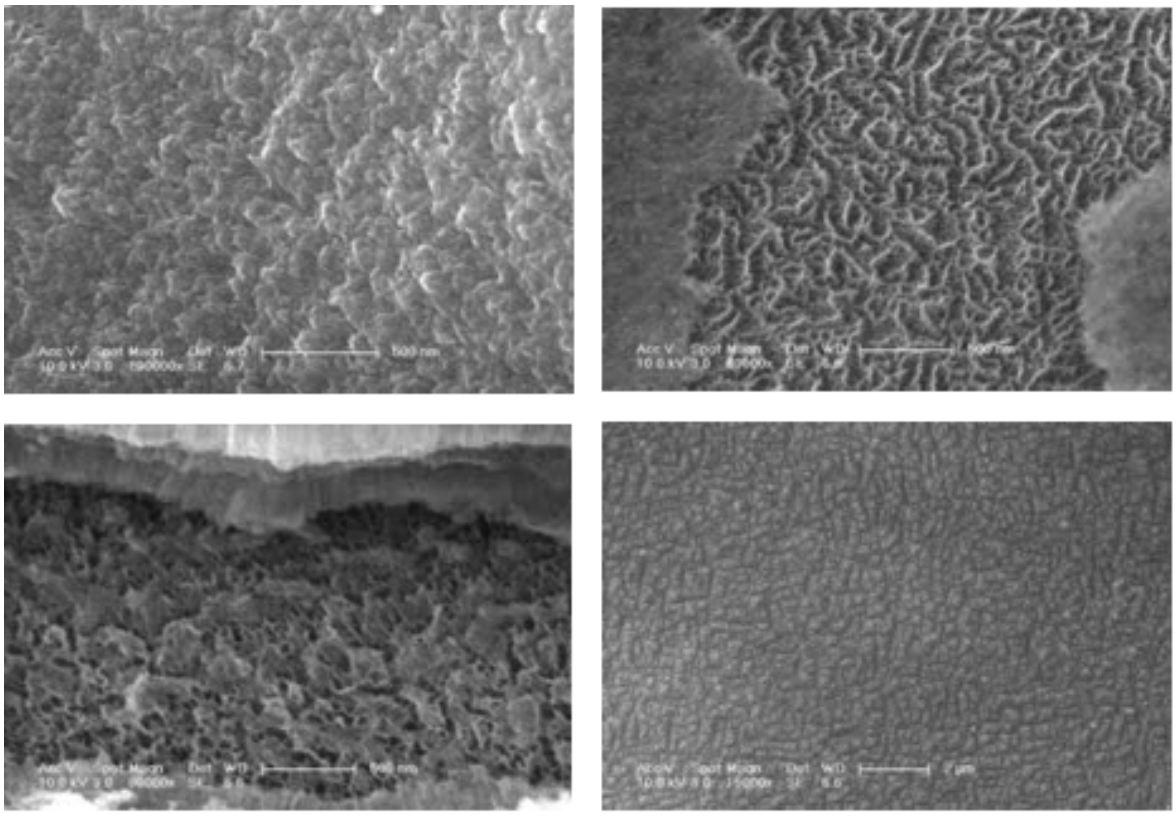

Figure 3.5. ESEM images of PS sample done by multi-mode laser

is attributed to the concentration of the doped materials in silicon. When it is doped with much more Boron, the concentration of positive charge carriers increases, also the current density increases according to the following equation

$$J = q(n\mu_n + p\mu_p)E \tag{3.1}$$

However, the current density must be within optimum limit [11].

Sample B is performed using single the tank cell with anodization time of 16 minutes. When it is looked at its photoluminescence, it is seen that there are two peaks wavelength at 620 nm and 667 nm . But, the PL graph of sample 10 has one peak intensity value at the wavelength of 675 nm.

There is also one more thing worth to mention. It is the anodization time difference between two anodization cells. In the basic anodization cell, anodization time differs from 30 minutes to 90 minutes while in the single tank cell, the anodization

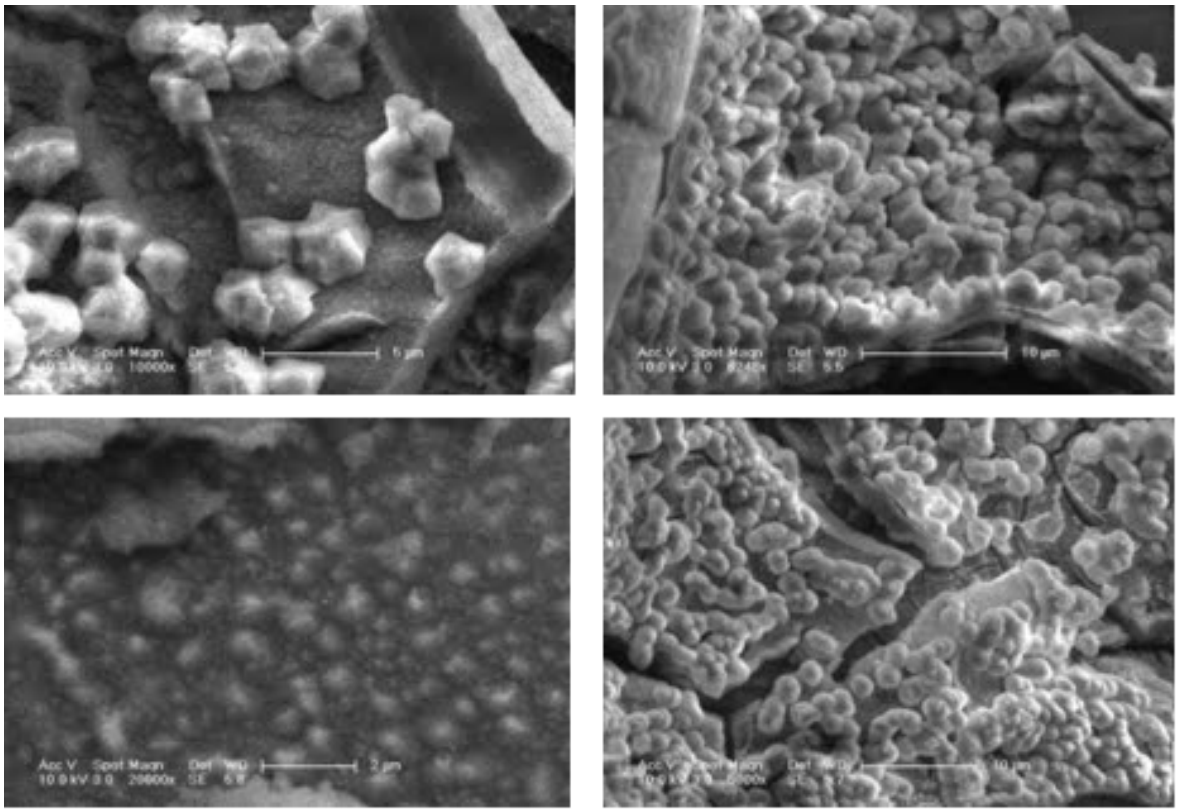

Figure 3.6. ESEM images of PS sample prepared by single-mode laser

time is roughly 10-20 minutes. The reason of the anodization time is being lower in the single tank cell is that the whole surface of the silicon sample is exposed to HF solution. After 30 minutes, the porous silicon sample in the single tank cell is burning and it does not have any nano-staructure layer.

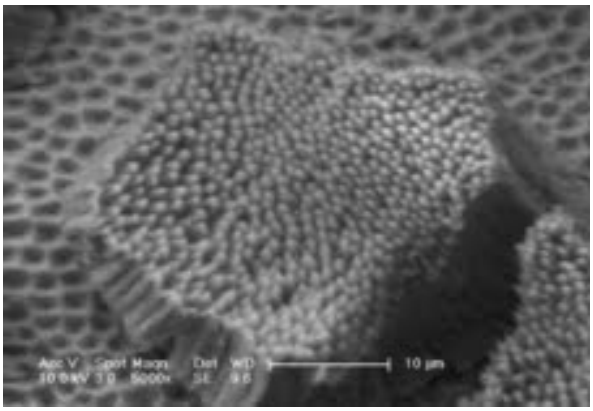

Figure 3.7. PS sample with low resistivity

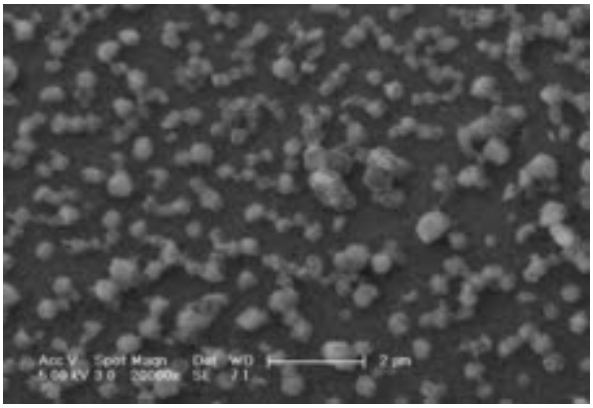

Figure 3.8. PS sample with high resistivity

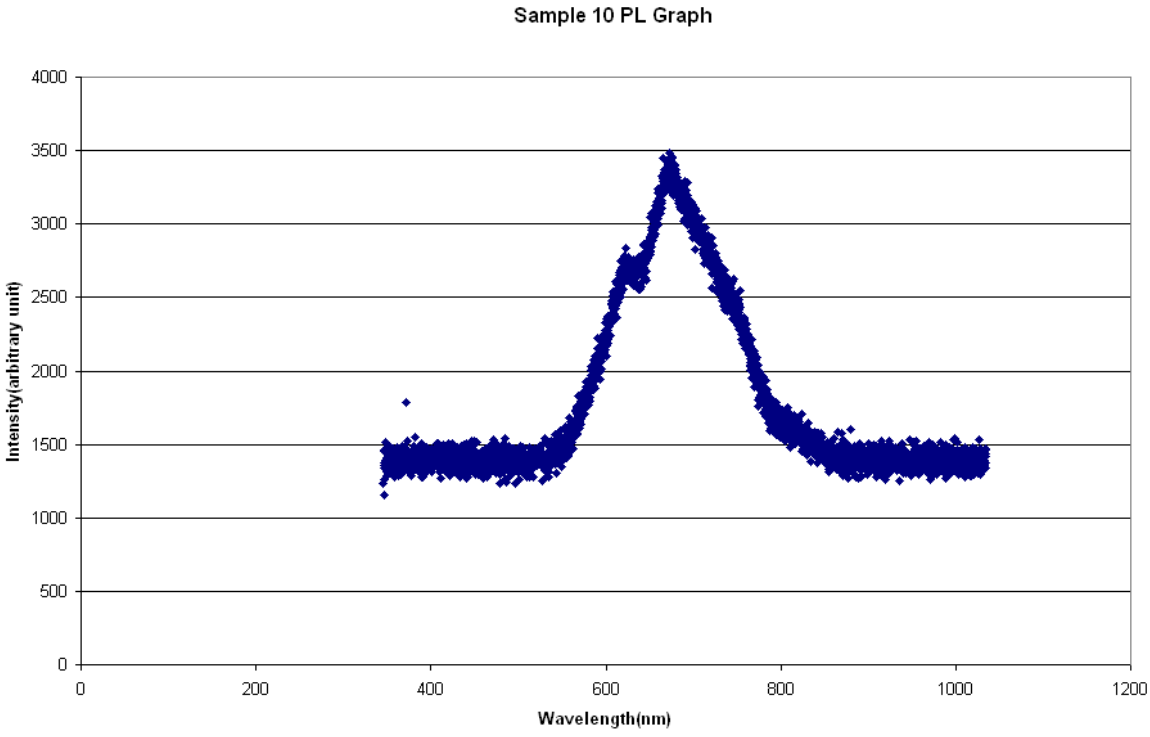

Figure 3.9. PS sample has a peak value of intensity at 675 nm

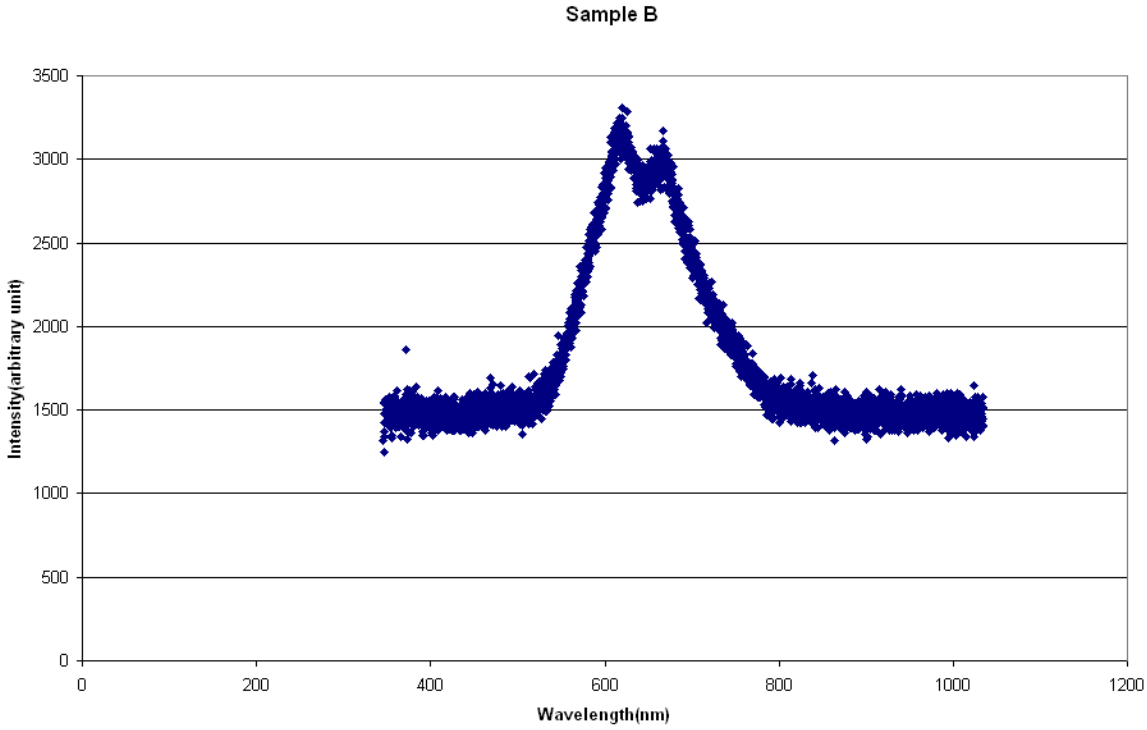

Figure 3.10. PS sample has peak value of intensity at 620 and 667 nm

4. Conclusion

In this thesis, porous silicon samples are prepared by two different anodization techniques which are the basic anodization cell and the single tank cell. Optical properties our samples are investigated by PL spectroscopy and their structural properties are investigated by ESEM.

Effecting parameters of porous silicon formation lies in the very large scale. The most important one is the resistivity. The resistivity effect of silicon on the formation of pores and pillars is examined by the ESEM images of PS samples.

Quantum confinement effect is observed by the help of optical characterization method, photoluminescence. PS samples having bigger pillar structure does not obey the rule of the quantum confinement effect. On the other hand, some PS samples have a dense pillar structure. Luminescence occurs at the sharp tips of the pillars since these tips are in the nanometer scale. Therefore, the quantum confinement effect is obtained through these tips.

For a future work, porosity of PS samples can be determined by different measurement techniques.

REFERENCES

1. Chen, B., J. Wei, F. H. T. , Francis, "Silicon Microneedle array with Biodegradable Tips for Transdermal Drug Delivery", *Microsyst Technol*, 14:1015-1019, 2008.

2. Menna P., G. D. Francia, V. L. Ferrara,"Porous Silicon in Solar Cells: A Review and a Description of Its Application as an AR Coating", *Solar Energy Materials and Solar Cells*, Vol 37, Issue 1, 1995.

3. Streetmen B., G., Banerjee, S., K., *Solid State Electronic Devices*, Prentice Hall, New Jersey, 2010.

4. Canham, L., *Properties of Porous Silicon*, Institution of Engineering and Technology, 1997.

5. Ossicini S., L. Pavesi, F. Priolo, "Light Emitting Silicon for Microphotonics", Springer, 2003.

6. Mathew F. P. , E. C. Alocilja, "Porous Silicon-based Biosensor for Pathogen Detection", *Biosensors and Bioelectronics*, 2005.

7. Pichonat T., B. G. Manuel, D. Hauden, "A New Photon-conducting Porous Silicon Membrane for Small Fuel Cells", *Chemical Engineering Journal*, 2004.

8. Chazalviel, J. N., R. B. Wehrspohn and F. Ozanam, "Electrochemical Preparation of Porous Semiconductors: from Phenomenology to Understanding", *Material Science and Engineering*, B69-70, 1-10, 2000.

9. Kasap, S. O., *Optoelectronics and Photonics. Principles and Practices*, Prentice Hall, New Jersey, 2001.

10. Rhoderick, E. H., *Metal-Semiconductor Contacts*, Clarendon, Oxford, 1978.

11. Saha, H., S. K. Dutta, S. M. Hossain, S. Chakraborty, A. Saha, "Mechanism and Control of Formation of Porous Silicon on p-type Si", *Indian Academy of Sciences*, Bull. Mater. Sci., Vol. 21, No. 3, pp. 195-201, June 1998.

12. Cahay M., *Quantum Confinement VI: Nanostructured Materials and Devices: Proceedings of the International Sypmposium*, Electrochemical Society Staff, 2001.

13. Behrisch, R., *Sputtering by Particle Bombardment*, Springer, Berlin, 1981.

14. Milani S. D., R. S. Dariani, A. Mortezaali, V. Daadmehr, K. Robbie, "The Correlation of Morphology and Surface Resistance in Porous Silicon", *Journal of Optoelectronics and Advanced Materials*, Vol. 8, No. 3, p.1216-1220, June 2006.